Interleukin-6 Signaling Blockade Induces Regulatory Plasmablasts in Neuromyelitis Optica Spectrum Disorder

Akatani, Ritsu ; Chihara, Norio ; Hara, Atsushi ; Tsuji, Asato ; Koto, Shusuke ; Kobayashi, Kazuhiro ; Toda, Tatsushi ; Matsumoto, Riki

(Citation)
NEUROLOGY® NEUROIMMUNOLOGY & NEUROINFLAMMATION,11(4):e200266

(Issue Date)
2024-06-18

(Resource Type)
journal article

(Version)
Version of Record

(URL)
https://hdl.handle.net/20.500.14094/0100490266

RESEARCH ARTICLE OPEN ACCESS

Interleukin-6 Signaling Blockade Induces Regulatory Plasmablasts in Neuromyelitis Optica Spectrum Disorder

Ritsu Akatani, MD, PhD, Norio Chihara, MD, PhD, Atsushi Hara, MD, PhD, Asato Tsuji, MD, Shusuke Koto, MD, PhD, Kazuhiro Kobayashi, PhD, Tatsushi Toda, MD, PhD, and Riki Matsumoto, MD, PhD

Correspondence
Dr. Chihara
chiharan@med.kobe-u.ac.jp

Neurol Neuroimmunol Neuroinflamm 2024;11:e200266. doi:10.1212/NXI.0000000000200266

Abstract

Background and Objectives

Interleukin-6 receptor antibodies (IL-6R Abs), including satralizumab, are increasingly used to prevent relapse for neuromyelitis optica spectrum disorder (NMOSD). However, the detailed mechanism of action of this treatment on the lymphocyte phenotype remains unclear. This study focused on B cells in patients with NMOSD, hypothesizing that IL-6R Ab enables B cells to acquire regulatory functions by producing the anti-inflammatory cytokine IL-10.

Methods

Peripheral blood mononuclear cells were stimulated in vitro to induce the expansion of B-cell subsets, double-negative B cells (DNs; $CD19^+$ IgD^-, $CD27^-$) and plasmablasts (PBs; $CD19^+$, $CD27^{hi}$, $CD38^{hi}$). Whole B cells, DNs, or PBs were isolated after culture with IL-6R Ab, and IL-10 expression was quantified using quantitative PCR and a cytometric bead array. RNA sequencing was performed to identify the marker of regulatory PBs induced by IL-6R Ab.

Results

DNs and PBs were observed to expand in patients with NMSOD during the acute attacks. In the in vitro model, IL-6R Ab increased IL-10 expression in B cells. Notably, IL-10 expression increased in PBs but not in DNs. Using RNA sequencing, CD200 was identified as a marker of regulatory PBs among the differentially expressed upregulated genes. $CD200^+$ PBs produced more IL-10 than $CD200^-$ PBs. Furthermore, patients with NMOSD who received satralizumab had a higher proportion of $CD200^+$ PBs than patients during the acute attacks.

Discussion

Treatment with IL-6 signaling blockade elicited a regulatory phenotype in B cells and PBs. $CD200^+$ PBs may be a marker of treatment responsiveness in the context of NMOSD pathophysiology.

Introduction

Neuromyelitis optica spectrum disorder (NMOSD) is a rare autoimmune disease characterized by relapsing inflammation affecting predominantly the optic nerve, spinal cord, and brainstem. Autoantibodies directed against the water channel aquaporin-4 (AQP4) are believed to play a pivotal role in the pathogenesis of NMOSD.[1,2] Several reports revealed that B-cell subsets were altered in both peripheral blood mononuclear cells (PBMCs) and CSF in patients with NMOSD.[3-6] For example, high proportions of plasmablasts (PBs), a mature and differentiated B-cell subset, have been observed in the PBMCs and CSF of patients with

From the Division of Neurology (R.A., N.C., A.H., A.T., S.K., R.M.); Division of Molecular Brain Science (K.K.), Kobe University Graduate School of Medicine; and Department of Neurology (T.T.), Graduate School of Medicine, The University of Tokyo, Japan.

Go to Neurology.org/NN for full disclosures. Funding information is provided at the end of the article.

The Article Processing Charge was funded by the authors.

Glossary

AQP4 = aquaporin-4; **ARR** = annualized relapse rate; **AZA** = azathioprine; **Ab** = antibody (or antibodies); **BCDT** = B cell depletion therapy; **Breg** = regulatory B cells; **CD** = cluster of differentiation; **DNs** = double negative B cells; **EAE** = experimental autoimmune encephalomyelitis; **EDSS** = Expanded Disability Status Scale; **EDTA** = ethylenediaminetetraacetic acid; **FACS** = fluorescence activated cell sorting; **FBS** = fetal bovine serum; **IL-6R** = IL-6 receptor; **IL-** = interleukin-; **Ig** = immunoglobulin; **MACS** = magnetic-activated cell sorting; **MEMs** = memory B cells; **MMF** = mycophenolate mofetil; **MTX** = methotrexate; **NAVs** = naïve B cells; **NMOSD** = neuromyelitis optica spectrum disorder; **PBMCs** = peripheral blood mononuclear cells; **PBS** = phosphate buffered saline; **PBs** = plasmablasts; **PCs** = plasma cells; **PMA** = phorbol-12-myristate-13-acetate; **PSL** = prednisolone; **RNA-seq** = RNA sequencing; **RPMI** = Roswell Park Memorial Institute; **SWMs** = switched memory B cells; **TAC** = tacrolimus; **Treg** = regulatory T cells; **USMs** = unswitched memory B cells; **cDNA** = complementary deoxyribonucleic acid; **qPCR** = quantitative polymerase chain reaction.

NMOSD and are associated with disease activity.[3] In addition, elevated interleukin (IL)-6 levels in both serum and CSF highlight its detrimental role in the underlying NMOSD pathophysiology[7,8] and its significance as a survival factor for PBs that produce anti-AQP4 antibodies.[3]

Based on these findings, randomized placebo-controlled trials with satralizumab, a humanized monoclonal antibody targeting the IL-6 receptor (IL-6R), have been successfully conducted to prevent NMOSD relapse.[9,10] Because IL-6 is a pleiotropic cytokine that plays a key role in several biological processes,[11] it remains elucidated how IL-6R signaling blockade alters lymphocyte phenotypes in patients with NMOSD. In addition, the criteria for appropriate patient selection for satralizumab or other therapies are not established, and specific biomarkers are needed. IL-6 was originally identified as a cytokine promoting the differentiation of B cells into antibody-secreting cells.[12] However, IL-6R blockade therapy does not completely abolish B-cell differentiation in vivo. Instead, it promotes the secretion of several cytokines from B cells in patients with rheumatoid arthritis receiving tocilizumab, another anti-IL-6R monoclonal antibody.[13]

This study aimed to investigate the hypothesis that disruption in regulatory B cells (Bregs) contributes to the pathogenesis of NMOSD and that their function can be restored by IL-6R blockade therapy. Bregs are commonly characterized cells that secrete the anti-inflammatory cytokine IL-10.[14] However, the role of Bregs in the pathogenesis of NMOSD and their association with IL-6R blockade therapy remain unknown. To clarify them, first, we performed longitudinal analysis of peripheral blood B cells from patients with NMOSD. This analysis revealed an expansion of B-cell subsets, such as double-negative B cells (DNs) and PBs, during acute disease flares and a subsequent decrease during remission. Second, using an in vitro model, we found that IL-6R blockade boosted the IL-10 expression of whole B cells and PBs, but not of DNs. Finally, we identified CD200 as a potential marker of regulatory PBs and validated its clinical relevance in patients with NMOSD treated with IL-6R blockade.

Methods

Participants and Specimens

A total of 31 patients with NMOSD who visited Kobe University Hospital between 2018 and 2023 were recruited for this study. Diagnosis of NMOSD was based on the 2015 criteria,[15] and all patients were seropositive for AQP4-IgG. Thirty-three age-matched and sex-matched healthy controls (HC) were also recruited. Baseline characteristics of patients with NMOSD and healthy controls are provided in eTable 1. A sample size calculation was performed to compare the means of the 2 groups. We set α error at 0.05, power (1-β) at 0.8, the difference in means between the 2 groups at 5%, and the SD common to the 2 groups at 5%, and the number of cases required was 16 for each group. The term "attack" used in this study refers to acute disease flares, as confirmed by both clinical and radiologic evidence. During attacks, samples were collected before initiating treatment, such as IV methylprednisolone or plasma exchange therapy. Remission was determined clinically and radiologically, basically under treatment including immunosuppressants. The clinical information of patients with NMOSD who received satralizumab is presented in eTable 2.

Standard Protocol, Approvals, Registrations, and Patient Consents

This study was approved by the institutional ethics committee (No. 1381). All the participants provided written informed consent.

Flow Cytometry Analysis and Cell Sorting

PBMCs were isolated from whole blood by density centrifugation using Ficoll-Paque Plus (GE Healthcare, Uppsala, Sweden). Owing to the significant reduction in PB cell count after freeze-thaw cycles,[16] blood samples were isolated into fresh PBMCs within 24 hours of collection for analysis without cryopreservation. Total B cells were separated from PBMCs using anti-CD19 magnetic-activated cell sorting (MACS) according to the manufacturer's instruction (Miltenyi Biotec, Bergisch Gladbach, Germany). PBMCs were stained with anti-human antibodies listed in eTable 3. Dead cells were excluded using Fixable Viability Dye eFluor 506 (Thermo Fisher Scientific, Waltham, MA). Flow cytometry

data were acquired using BD FACSVerse and LSRFortessa X-20, and cells were sorted by FACSAriaIII and FACSMelody (BD Biosciences, Franklin Lakes, NJ) and analyzed with FlowJo v10.8.1 (BD Biosciences).

IL-10 expression in B cells was assessed using a cytokine secretion assay in accordance with previous reports[17]; the IL-10 Secretion Assay Detection Kit (Miltenyi Biotec) was used according to the manufacturer's instructions. In brief, the cells were resuspended in the Roswell Park Memorial Institute (RPMI) 1640 medium at 1×10^6 cells/mL, and activation with phorbol-12-myristate-13-acetate (PMA; 20 ng/mL, Sigma-Aldrich, St. Louis, MO) and ionomycin (500 ng/mL, Sigma-Aldrich) was performed for 4 hours at 37°C. After washing with MACS buffer (PBS + 0.5% bovine serum albumin + 2 mM EDTA), the cells were resuspended in 90 μL of RPMI-1640 medium and mixed with 10 μL of IL-10 catch reagent for 5 minutes on ice. After rotation at 37°C for 45 minutes and washing with cold MACS buffer, the cells were stained with IL-10 detection antibody (PE) and antibodies for other cell surface molecules before analysis.

To quantify cytokine and immunoglobulin levels of culture supernatants, we used LEGENDplex Human Inflammation Panel 1 (13-plex) and LEGENDplex Human Immunoglobulin Isotyping Panel (8-plex) with a V-bottom plate (BioLegend), respectively, according to the manufacturer's instructions. In brief, culture supernatants (25 μL/sample) were incubated with capture beads for 2 hours at room temperature on a plate shaker. Next, the detection antibody was added, and the beads were incubated for 1 hour at room temperature on a plate shaker. After incubation with fluorescent antibodies, the beads were shaken for 30 minutes, washed, and analyzed using an LSRFortessa X-20 flow cytometer (BD Biosciences). Cytokine concentration was calculated based on a standard curve using BioLegend's LEGENDplex data analysis software.

Culture Assays

PBMCs were cultured in the RPMI-1640 medium supplemented with 10% heat-inactivated fetal bovine serum (FBS), 100 U/mL penicillin, and 100 μg/mL streptomycin in 96-well U-bottom plates at 37°C for 7 days. PBMCs were plated at a density of 2×10^5 cells/200 μL/well and stimulated with a cytokine cocktail comprising R848 (1 μg/mL, Enzo Lifesciences, Farmingdale, NY), IL-2 (50 ng/mL, PeproTech, Cranbury, NJ), CD40 ligand (50 ng/mL, R&D, Minneapolis, MN, USA), TNFα (1 ng/mL, PeproTech), IL-1β (1 ng/mL, PeproTech), and IL-21 (50 ng/mL, PeproTech). This cocktail was previously reported to induce in vitro production of AQP4-IgG from PBMCs of patients with NMOSD.[18] To assess the effect of IL-6R blockade, PBMCs were preincubated with either anti-IL-6 receptor antibody (1 μg/mL, R&D) or isotype control (1 μg/mL, R&D) on ice for 20 minutes. Subsequently, PBMCs were stimulated with the cytokine cocktail described above in addition to recombinant human IL-6 (1 ng/mL, R&D).

Real-Time Quantitative PCR and RNA Sequencing

Total RNA was isolated and purified from sorted cells using RNeasy Plus Mini Kit (QIAGEN, Hilden, Germany). Complementary DNA (cDNA) was synthesized from total RNA using SuperScript IV VILO Master Mix (Thermo Fisher Scientific). PCR primers designed in this study are listed in eTable 4. Real-time quantitative PCR (qPCR) was performed using CFX Connect (BioRad, Hercules, CA). The relative expressions of each mRNA were normalized to those of actin β (ACTB).

For RNA sequencing (RNA-seq) of differentiated PBs in vitro, PBMCs were isolated from 4 healthy controls and stimulated in vitro using the cytokine cocktail described above. PBs ($CD3^-$, $CD19^+$, $CD27^{hi}$, and $CD38^{hi}$) were sorted using FACSAriaIII (BD Biosciences). Total RNA was isolated and purified from the sorted PBs using RNeasy Mini Kit (Qiagen). RNA-seq libraries were generated using SMARTer Ultra Low RNA Kit (Takara Bio USA, Inc. San Jose, CA). The cDNA libraries were sequenced at a 100-bp paired-end on an Illumina Novaseq 6000 sequencer (Illumina, San Diego, CA). Sequencing run and the base-call analysis were performed according to the Novaseq 6000 System Guide with TruSeq library construction. RNA-seq reads were mapped to the hg38 genome using STAR-2.7.3a. Data were normalized using CPM (counts per million). Differentially expressed genes (DEGs) and heatmap figures were generated using gene-specific analysis (unadjusted p value < 0.05). Raw data processing and subsequent analysis were performed using software Partek Flow 7.0 (Partek Inc., Chesterfield, MO). Details of the chemicals and reagents used in these experiments are listed in eTable 5.

Statistical Analysis

Statistical analyses were conducted using GraphPad Prism v10.0.2 (GraphPad Software, Boston, MA). Detailed data analysis methods are described in the respective figure legends.

Data Availability

Anonymized data not published within this article will be made available by request from any qualified investigator.

Results

DNs and PBs Expand in the Acute Phase of NMOSD and Decrease in the Remission Phase

First, we performed longitudinal B-cell phenotyping analysis of patients with NMOSD. The proportion of double-negative B cells (DNs; $CD3^-$, $CD19^+$, IgD^-, $CD27^-$) and plasmablasts (PBs; $CD3^-$, $CD19^+$, $CD27^{hi}$, $CD38^{hi}$) within B cells in patients with NMOSD during acute attacks expanded compared with healthy controls (HC) (Figure 1A-B). The proportion of whole B cells to total lymphocytes had no difference (eFigure 1A). In addition, the proportion of switched

Figure 1 Increased Proportion of DNs and PBs in the Acute Phase of NMOSD Attacks and Their Changes Over Time

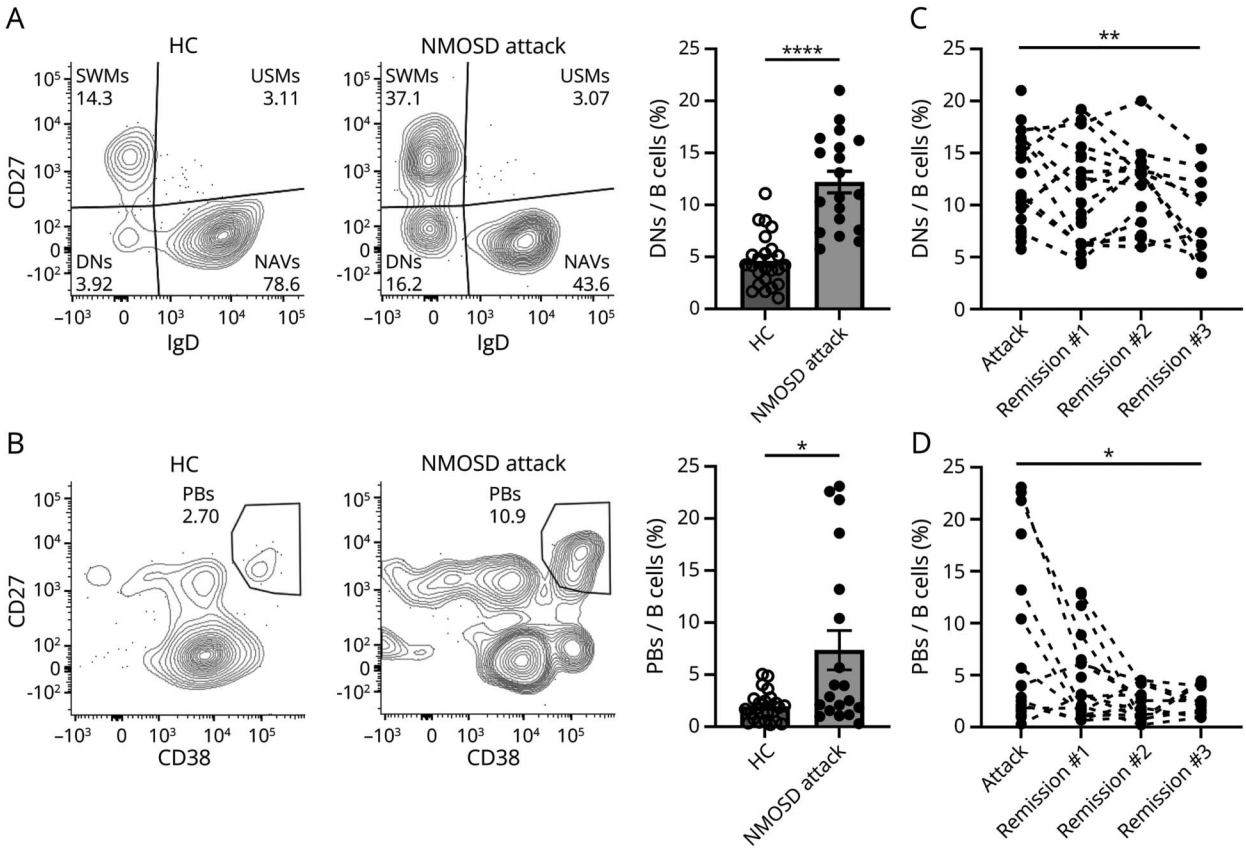

(A) Left: Representative flow cytometry analysis of DNs ($CD3^-$, $CD19^+$, IgD^-, $CD27^-$) from healthy controls (HC) and patients with NMOSD. The numbers in the areas represent percentages of the population. Right: Proportion of DNs. The open and filled symbols represent PBMC data obtained from 23 HC and 19 patients with acute NMOSD attacks, respectively (****$p < 0.0001$; Mann-Whitney test, the bar charts represent mean ± SEM). (B) Left: Representative flow cytometry analysis of PBs ($CD3^-$, $CD19^+$, $CD27^{hi}$, and $CD38^{hi}$) from HC and patients with NMOSD. Right: Proportion of PBs from 23 HC and 19 patients with NMOSD (*$p < 0.05$; Mann-Whitney test). (C, D) Longitudinal analysis of DNs and PBs. Dashed lines indicate that the samples are from the same patient. The mean interval between attack and remission #1 was 11.3 months (range 5–33). Sampling intervals for remissions #1, #2, and #3 were generally set at 6 months (**$p < 0.01$, *$p < 0.05$; fixed-effect p value, mixed-effect model; attack, n = 19; remission #1, n = 21; remission #2, n = 15; remission #3, n = 10). For cases experiencing relapse during the observation period, data acquired before the relapse were excluded because these showed an increase in PBs during the relapse compared with before, aligning the data with the attack as the first time point. DNs = double-negative B cells; HC = healthy controls; NMOSD = neuromyelitis optica spectrum disorder; PBs = plasmablasts. *$p < 0.05$, **$p < 0.01$, ***$p < 0.001$, and ****$p < 0.0001$.

memory B cells (SWMs; $CD3^-$, $CD19^+$, IgD^-, $CD27^+$) was higher while the proportion of naïve B cells (NAVs; $CD3^-$, $CD19^+$, IgD^+, $CD27^-$) was lower in patients with NMOSD compared with healthy controls (eFigure 1B). When clinical remission was reached, both DNs and PBs decreased. Of note, even during remission, proportions of both DNs and PBs remained high and gradually decreased over time to approach the levels observed in healthy controls (Figure 1, C and D). Moreover, we found that the expansion of DNs reflects the expansion of both double-negative 1 cells (DN1; $CD3^-$, $CD19^+$, IgD^-, $CD27^-$, $CXCR5^+$, $CD11c^-$) and double-negative 2 cells (DN2; $CD3^-$, $CD19^+$, IgD^-, $CD27^-$, $CXCR5^-$, $CD11c^+$), which are reciprocal DN subsets (eFigure 2A-B). While DN2 has been reported to expand in systemic lupus erythematosus as a precursor of autoantibody-producing cells,[19] no apparent difference was found in the ratio of DN1 or DN2 within the DNs in patients with NMOSD (eFigure 2, C–E). Furthermore, we investigated patients with NMOSD treated with satralizumab, which is an IL-6R antibody (Ab) drug, suggesting that the proportions of whole B cells, DNs, and PBs did not significantly alter (eFigure 3). These findings raised the possibility that IL-6R Ab may alter the B-cell phenotype as a treatment effect rather than the number of B cells or their canonical subsets.

IL-6R Blockade Induces *IL10* Expression in Whole B Cells and PBs But Not in DNs

Along with the observation of altered B-cell subsets during attacks, we stimulated PBMCs obtained from healthy controls and patients with NMOSD in the remission phase as an in vitro model of an attack. After 7 days of stimulation, DNs and PBs exhibited marked expansion, resembling the B-cell phenotypes observed during attacks (Figure 2A). Then, we purified B cells after stimulation and performed qPCR for *IL10* mRNA to determine whether IL-6R Ab treatment induces regulatory functions in B cells. IL-6R Ab increased the expression of *IL10* in B cells from PBMCs of both healthy controls and patients with NMOSD (Figure 2B, left). Of note,

Figure 2 In Vitro IL-6R Blockade Induces *IL10* Expression in Whole B Cells and PBs But Not in DNs

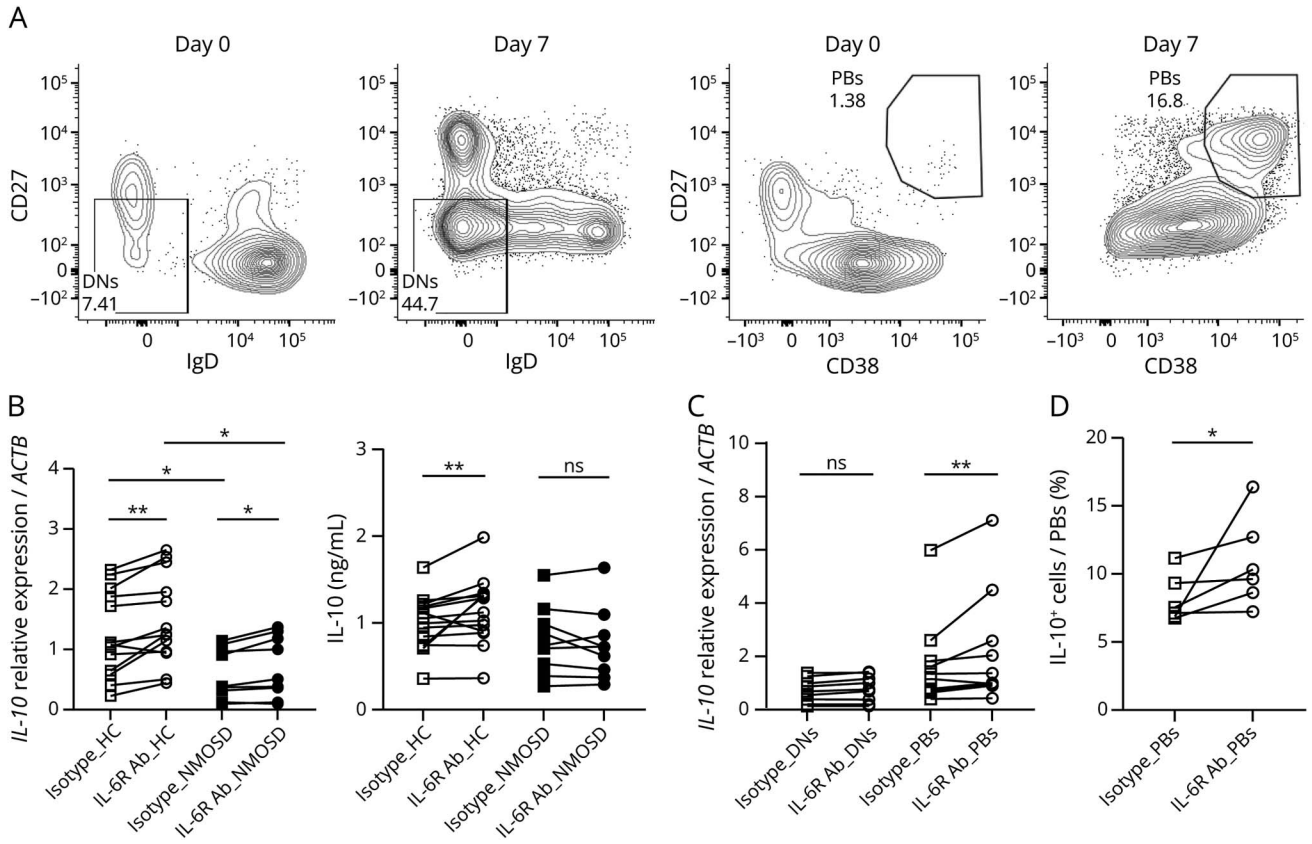

(A) Representative flow cytometry analysis before and after in vitro stimulation with PBMCs from HC. Both DNs and PBs expand on stimulation. (B) Left: Relative expression of *IL10* in B cells from 13 HC and 13 patients with NMOSD, with IL-6R Ab or isotype controls quantified by real-time qPCR (IL-6R Ab vs isotype; $^{**}p < 0.01$, $^{*}p < 0.05$; Wilcoxon matched-pairs signed-rank test; HC vs NMOSD; $^{*}p < 0.05$, Mann-Whitney test). Right: Levels of IL-10 in the culture supernatant measured by the cytometric bead array ($^{**}p < 0.01$; Wilcoxon matched-pairs signed-rank test). (C) Relative expression of *IL10* in DNs and PBs from 11 HC with IL-6R Ab or isotype controls. (D) Proportion of IL-10^{+} cells in induced PBs from PBMCs of 6 HC with IL-6R Ab or isotype controls, which is obtained using the cytokine secretion assay ($^{*}p < 0.05$; Wilcoxon matched-pairs signed-rank test). Data are from 3 or more independent experiments. ACTB = actin β; DNs = double-negative B cells; HC = healthy controls; IL-10 = interleukin-10; IL-6R Ab = IL-6 receptor antibody; NMOSD = neuromyelitis optica spectrum disorder; PBs = plasmablasts.

baseline *IL10* expressions of B cells were lower in patients with NMOSD compared with healthy controls (Figure 2B, left). In addition, IL-6R Ab elevated IL-10 protein levels in culture supernatants from healthy controls, but this difference was merely observed in patients with NMOSD (Figure 2B, right). The cytokine secretion assay further confirmed an elevation in the proportion of IL-10^{+} cells within B cells (eFigure 4A).

Next, to determine which B-cell subset elicited this regulatory response, we separated DNs and PBs and performed qPCR for *IL10* mRNA. IL-6R Ab increased *IL10* expression in PBs, but not in DNs (Figure 2C), suggesting that IL-6R blockade induces a regulatory function within the underlying mechanism by which B cells differentiate into PBs. We found that IL-6R Ab enabled PBs to acquire IL-10–producing function by the cytokine secretion assay (Figure 2D). When using PBMCs derived from patients with NMOSD under satralizumab treatment, the in vitro response to additional IL-6R Ab was not clearly evident. However, PBs produced higher levels of IL-10 compared with non-PBs, similar to healthy controls (eFigure 4B).

Transcriptional Profiles Revealed CD200 as a Marker of Regulatory PBs

Next, we performed global gene expression analysis on PBs expanded in vitro to search for additional markers that could characterize regulatory PBs. Using sorted PBs differentiated from 4 healthy controls, 593 DEGs were identified by comparing the IL-6R Ab treatment group with the isotype control group (Figure 3A). In these DEGs, we focused on 133 upregulated genes in the IL-6R Ab treatment group, including *IL10*. When systematically searching for potential cell surface markers, *CD200, TXK, SLC9A3*, and *TMEM11* emerged. We selected *CD200* for further investigation. Although CD200 is known as an inhibitory molecule in the context of inflammation, its role in NMOSD is unknown. Among PBMCs in a homeostatic state, B cells predominantly express CD200 compared with non-B cells (Figure 3B, left) and naïve B cells predominantly express CD200 among B-cell subsets

Figure 3 Transcriptional Profiles Showing CD200 as a Candidate for Regulatory PBs

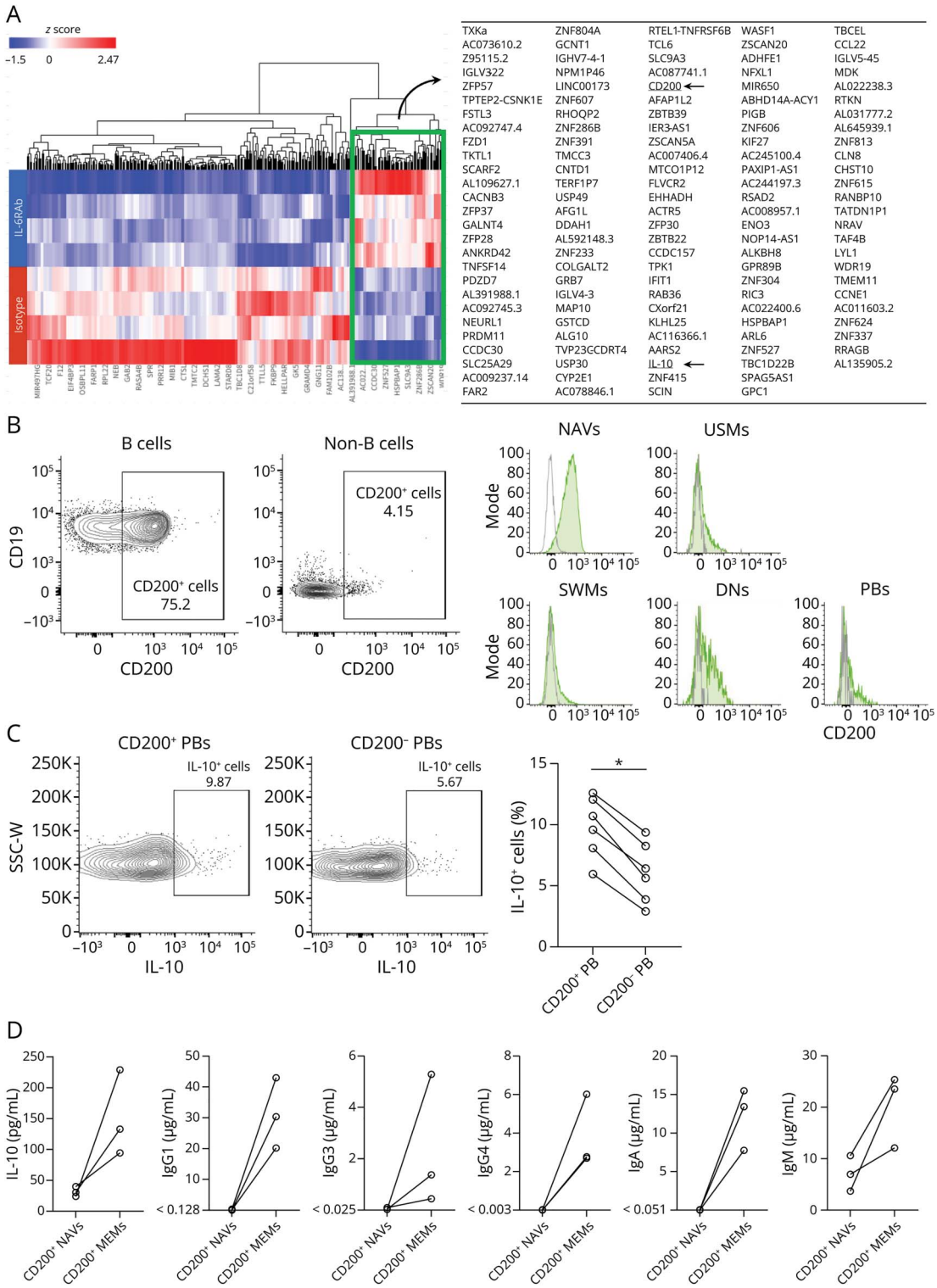

(A) Differential expression analysis with RNA-seq data from PBs induced by in vitro stimulation with IL-6R Ab or isotype control. The heatmap shows expression levels of sorted PBs derived from stimulated PBMCs of healthy controls (HC) (n = 4). The color intensity represents the column Z score, with red indicating high expression and blue indicating low expression. The regions outlined in green squares are transcripts upregulated by IL-6R Ab, and their contents are listed on the right. (B) Left: Representative flow cytometry analysis of CD200 expression in circulating B cells and non-B cells of HC. Most B cells express CD200 (75.2%), whereas most non-B cells do not (4.15%). Right: CD200 expression on canonical B-cell subsets. The gray lines indicate negative expression based on samples of fluorescence minus one. (C) Representative flow cytometry analysis and proportions of IL-10–producing cells within $CD200^+$ PBs compared with $CD200^-$ PBs based on the cytokine secretion assay (samples from HC, n = 6, $*p < 0.05$; Wilcoxon matched-pairs signed-rank test). (D) IL-10 and immunoglobulin quantification of culture supernatants from $CD200^+$ NAVs and $CD200^+$ MEMs from 3 HC. Samples below the detection sensitivity described on the y-axis are marked as 0. DNs = double-negative B cells; HC = healthy controls; IL-10 = interleukin-10; IL-6R Ab = IL-6 receptor antibody; MEMs = memory B cells; NAVs = naïve B cells; PBs = plasmablasts; SWMs = switched memory B cells; USMs = unswitched memory B cells.

(Figure 3B, right). To elucidate IL-10 production capacity of CD200$^+$ PBs, we performed the cytokine secretion assay and revealed that induced CD200$^+$ PBs tended to produce more IL-10 than CD200$^-$ PBs (Figure 3C), suggesting that CD200 might be a cell surface marker of regulatory PBs.

CD200$^+$ PB Are Predominantly Inducible From the Memory Phenotype

In addition, we purified 2 subfractions of B cells: CD200$^+$ naïve (CD3$^-$, CD19$^+$, IgD$^+$, CD27$^-$) and CD200$^+$ memory B cells (MEMs; CD3$^-$, CD19$^+$, CD27$^+$). Each group was stimulated separately to determine the B-cell subset from which CD200$^+$ PBs were induced. Both CD200$^+$ NAVs and CD200$^+$ MEMs differentiated into PBs in response to stimulation. CD200$^+$ MEMs produced more IL-10 and immunoglobulin isotypes than CD200$^+$ NAVs did (Figure 3D).

Circulating CD200$^+$ PBs in Patients With NMOSD and Their Relevance to Clinical Parameters

We performed cytokine secretion assays using PBMCs from patients with NMOSD, revealing higher IL-10 production capacity in CD200$^+$ PBs compared with CD200$^-$ PBs (Figure 4A). To assess the potential of circulating CD200$^+$ PBs in PBMCs as a cell subset representing Bregs induced by IL-6R Ab, we investigated its correlation with disease phases and relapse prevention therapies in patients with NMOSD. In PBMCs from patients with NMOSD, the proportion of CD200$^+$ PBs was significantly higher in the remission phase under satralizumab treatment than during attacks (Figure 4, B and C). In addition, all patients remained relapse-free after satralizumab administration. Of note, no significant difference was observed in CD200 expression in whole B cells or other subsets between the 2 groups (eFigure 5). Additional detailed analysis of the samples in the remission phase showed that CD200$^+$ PBs may be more likely to be induced in patients who experienced attacks within the past 12 months (Figure 4B, orange dots). This finding suggests a higher likelihood of CD200$^+$ PB induction during this specific period.

Finally, to determine the clinical characteristics of CD200$^+$ PBs in patients with NMOSD receiving satralizumab, we conducted a correlation analysis between age, disease duration, Expanded Disability Status Scale (EDSS) score, and

Figure 4 CD200+ PBs as Treatment Markers With Satralizumab for NMOSD

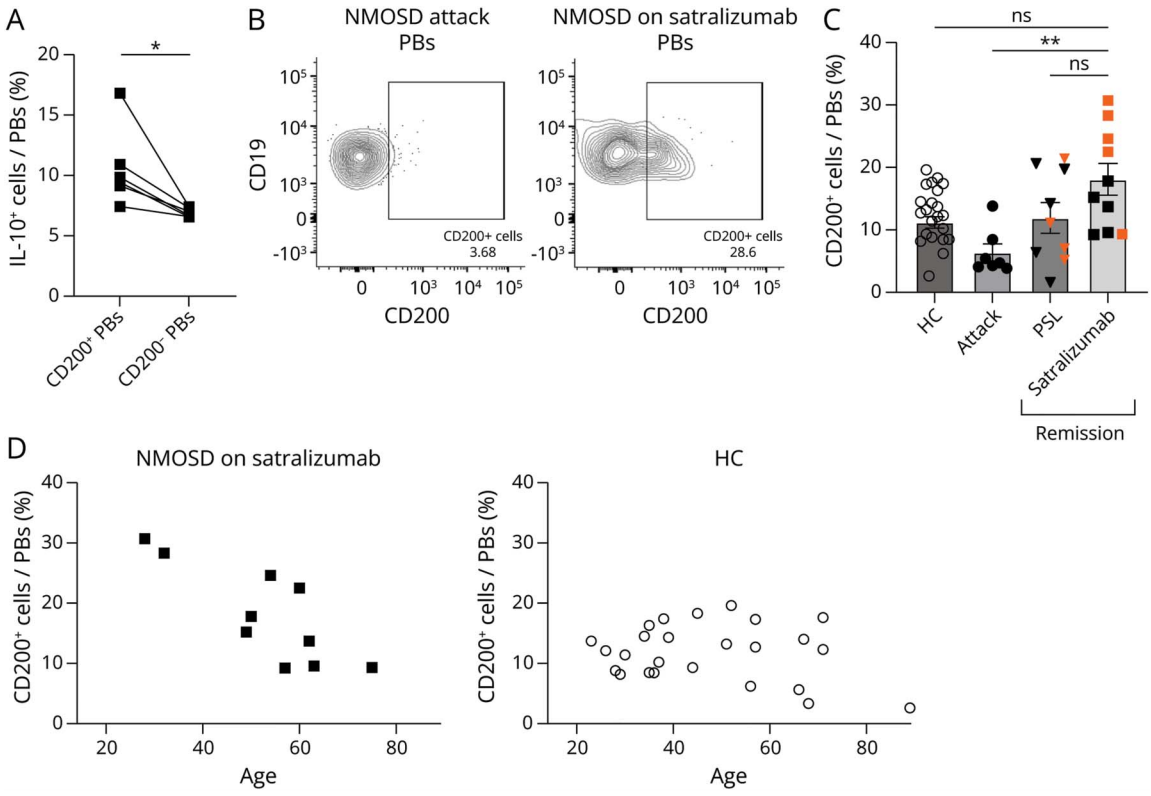

(A) Proportion of IL-10$^+$ cells in induced PBs from PBMCs of 6 patients with NMOSD with IL-6R Ab or isotype controls, which is obtained using the cytokine secretion assay (*p < 0.05; Wilcoxon matched-pairs signed-rank test). (B) Representative flow cytometry analysis of circulating CD200$^+$ cells in PBs. (C) Cumulative data show that PBs from patients with NMOSD receiving satralizumab in the remission phase have a higher percentage of CD200$^+$ cells compared with patients during an attack. PBMCs were obtained ≥4 months after initiating satralizumab treatment. Orange dots indicate samples taken <12 months after the most recent attack (HC; n = 28, attack; n = 7, remission on PSL; n = 9, remission on satralizumab; n = 10, **p < 0.01; Kruskal-Wallis test with Dunn multiple comparisons test). (D) Correlation between frequencies of CD200$^+$ PBs and age (NMOSD on satralizumab; n = 10, r = −0.7455, *p = 0.0174, HC; n = 28, r = −0.0312, p = 0.8747) (*p < 0.05; Spearman correlation, where r represents the correlation coefficient). HC = healthy controls; NMOSD = neuromyelitis optica spectrum disorder; PBs = plasmablasts; PSL = prednisolone.

annualized relapse rate (ARR) over the past 5 years. In patients receiving satralizumab, the proportion of CD200$^+$ PBs was negatively correlated with age. By contrast, this correlation was not evident in healthy controls (Figure 4D). These results suggest that patients receiving satralizumab might have a high propensity to develop CD200$^+$ PBs, especially among younger patients. Correlations between CD200$^+$ PBs and other clinical parameters are presented in eFigure 6.

Discussion

Our results demonstrate that IL-6R blockade induces a regulatory phenotype in B cells and that CD200$^+$ PBs may play a protective role in the pathophysiology of NMOSD. To date, several biologics have been developed based on the pathophysiology of NMOSD, generally aiming to deplete its pathogenic factors. For example, B-cell depletion therapy (BCDT), which targets the B-cell lineage marker CD19 or CD20, is an important treatment option for NMOSD.[20,21] However, some patients are resistant to BCDT for unknown reasons.[22,23] In animal models such as experimental autoimmune encephalomyelitis (EAE), contradictory data have been known to describe the complexity of BCDT; the depletion of B cells can result in clinical improvement or, conversely, exacerbation, which is dependent on the immunizing antigen and the timing of treatment.[24,25] Recently, it has also been implicated that BCDT not only depletes pathogenic B cells but also restores some subsets of Bregs.[26] These findings demonstrate the multifaceted nature of B cells, highlighting the importance of maintaining a balance between pathogenic and protective roles in NMOSD.

We found that *IL10* expression in stimulated B cells was lower in PBMCs from patients with NMOSD compared with those from healthy controls (Figure 2B, left), suggesting a disruption of the Breg induction system in NMOSD. Similar findings have been reported in some subsets of circulating Bregs in patients with NMOSD.[27-29] With IL-6R blockade, B cells acquired increased *IL10* expression in an in vitro model. Consistent with this finding, some reports showed that tocilizumab restores dysregulated cytokine production from B cells in patients with rheumatoid arthritis.[13,30] A similar mechanism may be involved in patients with NMOSD receiving satralizumab treatment.

Meanwhile, a previous study reported that serum AQP4-IgG titers did not change significantly with IL-6R blockade therapy.[31] These results suggest that B cells may shift from a pathogenic to a regulatory phenotype with satralizumab treatment, despite maintaining antigen specificity. This theory might be supported by the observation that relapses were milder in patients receiving long-term satralizumab treatment.[32] As an upstream mechanism of B-cell differentiation, IL-6 has been reported to inhibit regulatory T-cell (Treg) function and prevent Th17 cells from converting to Tregs.[33,34] Our findings of Breg induction by IL-6R blockade in PBMC culture might occur through these mechanisms.

Although it has been suggested that IL-10–producing B cells can be induced from multiple B-cell subsets on different stimuli,[35] PBs or plasma cells (PCs) have also been reported to have the ability to produce IL-10.[36-38] PCs are generally believed to divide infrequently, and a subset of PCs have the capacity to be extremely long-lived in tissue.[39] While circulating PBs constitute a minor fraction of PBMCs, they could represent PB/PCs in vivo, as B cells differentiate and function in secondary lymphoid tissues.[40] Sampling from these tissues might provide more detailed information.[41] The co-expression of CD200 in LAG3-positive natural regulatory PCs was described.[37] This finding potentially corresponds to the regulatory PBs observed in our study, although the PBs in our study were induced by in vitro stimulation.

In the context of autoimmunity, several reports suggest that CD200 acts in a disease-suppressive manner in animal models, including EAE.[42,43] Within the CNS, CD200 is expressed in neurons, astrocytes, and oligodendrocytes in a homeostatic state and is believed to negatively regulate CD200 receptor-positive microglia.[44] Furthermore, in the postmortem brain pathology of NMOSD, acute lesions demonstrate B-cell infiltration into the CNS,[45] and further studies are needed to elucidate how B cells or PBs with this phenotype behave inside the CNS.

The expansion of DNs and PBs observed during NMOSD attacks is consistent with a recent report using single-cell RNA-seq techniques.[46] By longitudinal analysis, we found that DNs and PBs exhibited a subsequent decrease after the attacks (Figure 1C-D), suggesting the importance of considering the clinical phase when analyzing the lymphocyte phenotype. Recent research on the clinical course of NMOSD has indicated that relapses are more likely to occur during an early period within 12 months of the last clinical attack.[47] Based on this report, we evaluated the CD200$^+$ PB proportion separately within or outside this period (Figure 4C). Of note, CD200$^+$ PBs expanded in this early period in patients with NMOSD receiving satralizumab, indicating that B-cell differentiation under disease activity is skewed toward the immune regulatory side that potentially becomes pathogenic in cases without treatment. While there is no established indicator to determine whether patients achieved a sufficiently low risk of relapse, efforts to explore this from an immunologic viewpoint are warranted.

This study has several limitations. When interpreting longitudinal data of clinical samples from patients with NMOSD, it is crucial to note the potential influence of various medications during acute and remission phases. We analyzed clinical samples from patients already diagnosed with NMOSD, and this analysis was not conducted considering the demographic background and previous medication status. Patients treated with biologics may have relatively high disease activity, and it should be noted that they may not reflect the entire NMOSD population. Given that patients receiving satralizumab may also represent relatively severe cases, this could be a reason for the observation that the proportions of DNs and PBs did not significantly decrease after the initiation of satralizumab

(eFigure 3). Furthermore, we have only demonstrated one aspect of IL-6 signaling blockade, focusing on IL-10 as a Breg marker. We could not elucidate the details of B-cell intrinsic mechanisms of IL-10 or CD200 induction by IL-6R Ab using functional assays. The PBs we observed may also only partially reflect the tissue responses occurring in vivo. Finally, the limited number of patients receiving satralizumab warrants attention to confounding factors in interpreting the correlation between $CD200^{+}$ PBs and clinical parameters, and the longitudinal assessment of each patient remains incomplete. Although further research is needed to fully explore these aspects, our current findings on regulatory PBs could contribute to the emerging field of Bregs in the pathophysiology of NMOSD.

Because NMOSD may require lifelong treatments to prevent relapses, curative therapy, including the restoration of self-tolerance, should be developed.[48-50] In the evolution of treatments for NMOSD from conventional immunosuppressive therapy to a curative therapy, precise and maximized restoration of disrupted regulatory systems is indispensable. The regulatory PBs found in our study might be one target for future therapies. Our findings suggest that the induction of regulatory PBs represents a novel mechanism of action for NMOSD treatment through the IL-6 signaling blockade. The role of Bregs in NMOSD remains poorly understood and requires further study, especially regarding their focal behavior (e.g., in the lymph nodes, spleen, bone marrow, and CNS) and interactions with other cells.

Acknowledgment

The authors thank the patients and healthy volunteers involved in this study. The authors also thank Masayuki Taniguchi from the Division of Pharmacology at Kobe University Graduate School of Medicine for advice on the RNA sequencing data analysis.

Study Funding

This study was funded by a Grant-in-Aid for Research Activity Start-up and a Grant-in-Aid for Early-Career Scientists from the Japan Society for the Promotion of Science (JSPS KAKENHI grant 21K20871 and 23K14778) (A.R.). A grant-in-aid for Scientific Research from the Japan Society for the Promotion of Science (20H03562 and 23H02797) (N.C.), Practical Research Project for Rare/Intractable Diseases by AMED (22ek0109436h0003) (N.C.), AMED CREST (22gm1710005h0001 and 23gm1710005h0002) (N.C.).

Disclosure

The authors report no relevant disclosures. Go to Neurology.org/NN for full disclosures.

Publication History

Received by *Neurology: Neuroimmunology & Neuroinflammation* January 22, 2024. Accepted in final form April 17, 2024. Submitted and externally peer reviewed. The handling editor was Deputy Editor Scott S. Zamvil, MD, PhD, FAAN.

Appendix Authors

Name	Location	Contribution
Ritsu Akatani, MD, PhD	Division of Neurology, Kobe University Graduate School of Medicine, Japan	Drafting/revision of the manuscript for content, including medical writing for content; major role in the acquisition of data; study concept or design; analysis or interpretation of data
Norio Chihara, MD, PhD	Division of Neurology, Kobe University Graduate School of Medicine, Japan	Drafting/revision of the manuscript for content, including medical writing for content; study concept or design; analysis or interpretation of data
Atsushi Hara, MD, PhD	Division of Neurology, Kobe University Graduate School of Medicine, Japan	Drafting/revision of the manuscript for content, including medical writing for content; major role in the acquisition of data
Asato Tsuji, MD	Division of Neurology, Kobe University Graduate School of Medicine, Japan	Drafting/revision of the manuscript for content, including medical writing for content; major role in the acquisition of data
Shusuke Koto, MD, PhD	Division of Neurology, Kobe University Graduate School of Medicine, Japan	Drafting/revision of the manuscript for content, including medical writing for content
Kazuhiro Kobayashi, PhD	Division of Molecular Brain Science, Kobe University Graduate School of Medicine, Japan	Drafting/revision of the manuscript for content, including medical writing for content
Tatsushi Toda, MD, PhD	Department of Neurology, Graduate School of Medicine, The University of Tokyo, Japan	Drafting/revision of the manuscript for content, including medical writing for content
Riki Matsumoto, MD, PhD	Division of Neurology, Kobe University Graduate School of Medicine, Japan	Drafting/revision of the manuscript for content, including medical writing for content

References

1. Lennon VA, Wingerchuk DM, Kryzer TJ, et al. A serum autoantibody marker of neuromyelitis optica: distinction from multiple sclerosis. *Lancet*. 2004;364(9451):2106-2112. doi:10.1016/S0140-6736(04)17551-X
2. Lennon VA, Kryzer TJ, Pittock SJ, Verkman AS, Hinson SR. IgG marker of optic-spinal multiple sclerosis binds to the aquaporin-4 water channel. *J Exp Med*. 2005;202(4):473-477. doi:10.1084/jem.20050304
3. Chihara N, Aranami T, Sato W, et al. Interleukin 6 signaling promotes anti-aquaporin 4 autoantibody production from plasmablasts in neuromyelitis optica. *Proc Natl Acad Sci U S A*. 2011;108(9):3701-3706. doi:10.1073/pnas.1017385108
4. Chihara N, Aranami T, Oki S, et al. Plasmablasts as migratory IgG-producing cells in the pathogenesis of neuromyelitis optica. *PLoS One*. 2013;8(12):e83036. doi:10.1371/journal.pone.0083036
5. Kowarik MC, Astling D, Gasperi C, et al. CNS Aquaporin-4-specific B cells connect with multiple B-cell compartments in neuromyelitis optica spectrum disorder. *Ann Clin Transl Neurol*. 2017;4(6):369-380. doi:10.1002/acn3.418
6. Hoshino Y, Noto D, Sano S, et al. Dysregulated B cell differentiation towards antibody-secreting cells in neuromyelitis optica spectrum disorder. *J Neuroinflammation*. 2022;19(1):6. doi:10.1186/s12974-021-02375-w
7. Uzawa A, Mori M, Arai K, et al. Cytokine and chemokine profiles in neuromyelitis optica: significance of interleukin-6. *Mult Scler*. 2010;16(12):1443-1452. doi:10.1177/1352458510379247
8. Uzawa A, Mori M, Sato Y, Masuda S, Kuwabara S. CSF interleukin-6 level predicts recovery from neuromyelitis optica relapse. *J Neurol Neurosurg Psychiatry*. 2012;83(3):339-340. doi:10.1136/jnnp.2011.241760
9. Yamamura T, Kleiter I, Fujihara K, et al. Trial of satralizumab in neuromyelitis optica spectrum disorder. *N Engl J Med*. 2019;381(22):2114-2124. doi:10.1056/NEJMoa1901747

10. Traboulsee A, Greenberg BM, Bennett JL, et al. Safety and efficacy of satralizumab monotherapy in neuromyelitis optica spectrum disorder: a randomised, double-blind, multicentre, placebo-controlled phase 3 trial. *Lancet Neurol.* 2020;19(5):402-412. doi:10.1016/S1474-4422(20)30078-8
11. Tanaka T, Narazaki M, Kishimoto T. IL-6 in inflammation, immunity, and disease. *Cold Spring Harb Perspect Biol.* 2014;6(10):a016295. doi:10.1101/cshperspect.a016295
12. Hirano T, Yasukawa K, Harada H, et al. Complementary DNA for a novel human interleukin (BSF-2) that induces B lymphocytes to produce immunoglobulin. *Nature.* 1986;324(6092):73-76. doi:10.1038/324073a0
13. Fleischer S, Ries S, Shen P, et al. Anti-interleukin-6 signalling therapy rebalances the disrupted cytokine production of B cells from patients with active rheumatoid arthritis. *Eur J Immunol.* 2018;48(1):194-203. doi:10.1002/eji.201747191
14. Mauri C, Menon M. Human regulatory B cells in health and disease: therapeutic potential. *J Clin Invest.* 2017;127(3):772-779. doi:10.1172/JCI85113
15. Wingerchuk DM, Banwell B, Bennett JL, et al. International consensus diagnostic criteria for neuromyelitis optica spectrum disorders. *Neurology.* 2015;85(2):177-189. doi:10.1212/WNL.0000000000001729
16. Kyu SY, Kobie J, Yang H, et al. Frequencies of human influenza-specific antibody secreting cells or plasmablasts post vaccination from fresh and frozen peripheral blood mononuclear cells. *J Immunol Methods.* 2009;340(1):42-47. doi:10.1016/j.jim.2008.09.025
17. Rezk A, Li R, Bar-Or A. Multiplexed detection and isolation of viable low-frequency cytokine-secreting human B cells using cytokine secretion assay and flow cytometry (CSA-Flow). *Sci Rep.* 2020;10(1):14823. doi:10.1038/s41598-020-71750-z
18. Wilson R, Makuch M, Kienzler AK, et al. Condition-dependent generation of aquaporin-4 antibodies from circulating B cells in neuromyelitis optica. *Brain.* 2018;141(4):1063-1074. doi:10.1093/brain/awy010
19. Jenks SA, Cashman KS, Zumaquero E, et al. Distinct effector B cells induced by unregulated toll-like receptor 7 contribute to pathogenic responses in systemic lupus erythematosus. *Immunity.* 2018;49(4):725-739.e6. doi:10.1016/j.immuni.2018.08.015
20. Damato V, Evoli A, Iorio R. Efficacy and safety of rituximab therapy in neuromyelitis optica spectrum disorders: a systematic review and meta-analysis. *JAMA Neurol.* 2016;73(11):1342-1348. doi:10.1001/jamaneurol.2016.1637
21. Cree BAC, Bennett JL, Kim HJ, et al. Inebilizumab for the treatment of neuromyelitis optica spectrum disorder (N-MOmentum): a double-blind, randomised placebo-controlled phase 2/3 trial. *Lancet.* 2019;394(10206):1352-1363. doi:10.1016/S0140-6736(19)31817-3
22. Perumal JS, Kister I, Howard J, Herbert J. Disease exacerbation after rituximab induction in neuromyelitis optica. *Neurol Neuroimmunol Neuroinflamm.* 2015;2(1):e61. doi:10.1212/NXI.0000000000000061
23. Dai Y, Lu T, Wang Y, et al. Rapid exacerbation of neuromyelitis optica after rituximab treatment. *J Clin Neurosci.* 2016;26:168-170. doi:10.1016/j.jocn.2015.08.033
24. Sefia E, Pryce G, Meier UC, Giovannoni G, Baker D. Depletion of CD20 B cells fails to inhibit relapsing mouse experimental autoimmune encephalomyelitis. *Mult Scler Relat Disord.* 2017;14:46-50. doi:10.1016/j.msard.2017.03.013
25. Häusler D, Häusser-Kinzel S, Feldmann L, et al. Functional characterization of reappearing B cells after anti-CD20 treatment of CNS autoimmune disease. *Proc Natl Acad Sci U S A.* 2018;115(39):9773-9778. doi:10.1073/pnas.1810470115
26. Kim Y, Kim SY, Han SM, et al. Functional impairment of CD19(+)CD24(hi) CD38(hi) B cells in neuromyelitis optica spectrum disorder is restored by B cell depletion therapy. *Sci Transl Med.* 2021;13(624):eabk2132. doi:10.1126/scitranslmed.abk2132
27. Quan C, Yu H, Qiao J, et al. Impaired regulatory function and enhanced intrathecal activation of B cells in neuromyelitis optica: distinct from multiple sclerosis. *Mult Scler.* 2013;19(3):289-298. doi:10.1177/1352458512454771
28. Han J, Sun L, Wang Z, et al. Circulating regulatory B cell subsets in patients with neuromyelitis optica spectrum disorders. *Neurol Sci.* 2017;38(7):1205-1212. doi:10.1007/s10072-017-2932-7
29. Matsuoka T, Araki M, Lin Y, et al. Long-term effects of IL-6 receptor blockade therapy on regulatory lymphocytes and neutrophils in neuromyelitis optica spectrum disorder. *Neurol Neuroimmunol Neuroinflamm.* 2024;11(1):e200173. doi:10.1212/NXI.0000000000200173
30. Snir A, Kessel A, Haj T, Rosner I, Slobodin G, Toubi E. Anti-IL-6 receptor antibody (tocilizumab): a B cell targeting therapy. *Clin Exp Rheumatol.* 2011;29(4):697-700.
31. Ringelstein M, Ayzenberg I, Harmel J, et al. Long-term therapy with interleukin 6 receptor blockade in highly active neuromyelitis optica spectrum disorder. *JAMA Neurol.* 2015;72(7):756-763. doi:10.1001/jamaneurol.2015.0533
32. Kleiter I, Traboulsee A, Palace J, et al. Long-term efficacy of satralizumab in AQP4-IgG-seropositive neuromyelitis optica spectrum disorder from SAkuraSky and SAkuraStar. *Neurol Neuroimmunol Neuroinflamm.* 2023;10(1):e200071. doi:10.1212/NXI.0000000000200071
33. Korn T, Mitsdoerffer M, Croxford AL, et al. IL-6 controls Th17 immunity in vivo by inhibiting the conversion of conventional T cells into Foxp3+ regulatory T cells. *Proc Natl Acad Sci U S A.* 2008;105(47):18460-18465. doi:10.1073/pnas.0809850105
34. Pasare C, Medzhitov R. Toll pathway-dependent blockade of CD4+CD25+ T cell-mediated suppression by dendritic cells. *Science.* 2003;299(5609):1033-1036. doi:10.1126/science.1078231
35. Glass MC, Glass DR, Oliveria JP, et al. Human IL-10-producing B cells have diverse states that are induced from multiple B cell subsets. *Cell Rep.* 2022;39(3):110728. doi:10.1016/j.celrep.2022.110728
36. Matsumoto M, Baba A, Yokota T, et al. Interleukin-10-producing plasmablasts exert regulatory function in autoimmune inflammation. *Immunity.* 2014;41(6):1040-1051. doi:10.1016/j.immuni.2014.10.016
37. Lino AC, Dang VD, Lampropoulou V, et al. LAG-3 inhibitory receptor expression identifies immunosuppressive natural regulatory plasma cells. *Immunity.* 2018;49(1):120-133.e9. doi:10.1016/j.immuni.2018.06.007
38. Rojas OL, Pröbstel AK, Porfilio EA, et al. Recirculating intestinal IgA-producing cells regulate neuroinflammation via IL-10. *Cell.* 2019;176(3):610-624.e18. doi:10.1016/j.cell.2018.11.035
39. Tellier J, Nutt SL. Plasma cells: the programming of an antibody-secreting machine. *Eur J Immunol.* 2019;49(1):30-37. doi:10.1002/eji.201847517
40. Pelletier N, McHeyzer-Williams LJ, Wong KA, Urich E, Fazilleau N, McHeyzer-Williams MG. Plasma cells negatively regulate the follicular helper T cell program. *Nat Immunol.* 2010;11(12):1110-1118. doi:10.1038/ni.1954
41. Damato V, Theorell J, Al-Diwani A, et al. Rituximab abrogates aquaporin-4-specific germinal center activity in patients with neuromyelitis optica spectrum disorders. *Proc Natl Acad Sci U S A.* 2022;119(24):e2121804119. doi:10.1073/pnas.2121804119
42. Hoek RM, Ruuls SR, Murphy CA, et al. Down-regulation of the macrophage lineage through interaction with OX2 (CD200). *Science.* 2000;290(5497):1768-1771. doi:10.1126/science.290.5497.1768
43. Liu Y, Bando Y, Vargas-Lowy D, et al. CD200R1 agonist attenuates mechanisms of chronic disease in a murine model of multiple sclerosis. *J Neurosci.* 2010;30(6):2025-2038. doi:10.1523/JNEUROSCI.4272-09.2010
44. Manich G, Recasens M, Valente T, Almolda B, González B, Castellano B. Role of the CD200-CD200R Axis during Homeostasis and neuroinflammation. *Neuroscience.* 2019;405:118-136. doi:10.1016/j.neuroscience.2018.10.030
45. Takai Y, Misu T, Suzuki H, et al. Staging of astrocytopathy and complement activation in neuromyelitis optica spectrum disorders. *Brain.* 2021;144(8):2401-2415. doi:10.1093/brain/awab102
46. Zhang C, Zhang TX, Liu Y, et al. B-cell compartmental features and molecular basis for therapy in autoimmune disease. *Neurol Neuroimmunol Neuroinflamm.* 2021;8(6):e1070. doi:10.1212/NXI.0000000000001070
47. Akaishi T, Nakashima I, Takahashi T, Abe M, Ishii T, Aoki M. Neuromyelitis optica spectrum disorders with unevenly clustered attack occurrence. *Neurol Neuroimmunol Neuroinflamm.* 2020;7(1):e640. doi:10.1212/NXI.0000000000000640
48. Steinman L, Bar-Or A, Behne JM, et al. Restoring immune tolerance in neuromyelitis optica: Part I. *Neurol Neuroimmunol Neuroinflamm.* 2016;3(5):e276. doi:10.1212/NXI.0000000000000276
49. Bar-Or A, Steinman L, Behne JM, et al. Restoring immune tolerance in neuromyelitis optica: part II. *Neurol Neuroimmunol Neuroinflamm.* 2016;3(5):e277. doi:10.1212/NXI.0000000000000277
50. Loda E, Arellano G, Perez-Giraldo G, Miller SD, Balabanov R. Can immune tolerance be re-established in neuromyelitis optica? *Front Neurol.* 2021;12:783304. doi:10.3389/fneur.2021.783304